MARTIAN DUST STORMS: A REVIEW *

WALTER FERNÁNDEZ
Laboratory for Atmospheric and Planetary Research, DFAOP/School of Physics and Centre for Geophysical Research, University of Costa Rica, San José, Costa Rica

(Received 11 February 1998; Accepted 20 October 1998)

Abstract. A review of the dust storms observed on Mars is made. This includes the seasonal and interannual variability of planet-encircling and regional dust storms. Although there is a significant interannual variability, planet-encircling dust storms have been observed to form during the southern spring and summer seasons, while regional dust storms tend to occur more frequently. Some aspects of possible mechanisms associated with the origin, maintenance and decay of the dust storms are also discussed.

1. Introduction

Although Mars and the Earth share some similarities (for example, axial tilt and rotation rate), they also show marked differences between them. On Mars, the dust raised from the surface into the atmosphere by strong winds absorbs solar radiation and constitutes an important internal heat source. In addition, on Mars the sublimation and condensation of carbon dioxide produces a mass flow from the subliming polar cap to the condensing polar cap. A comprehensive understanding of the Martian general atmospheric circulation requires knowledge of the processes which control the seasonal and interannual variations of the injection, transport and removal of dust, water vapor, and carbon dioxide (e.g., Zurek et al., 1992).

Planetary atmospheres offer many fascinating research topics. One of them is the Martian dust storms, also called Martian yellow storms or Martian yellow clouds. They have been observed for a long time (e.g., Antoniadi, 1930; Martin and Zurek, 1993). The planet-encircling dust storms appear to form when one or several local dust storm expand or when more than one dust storms expand and merge (e.g., Ebisawa and Dollfus, 1986). They obscure large areas on Mars from periods from days to months. The thermal structure of the atmosphere is modified by the dust and, consequently, the atmospheric circulation is also perturbed. Planet-encircling storms transport dust over long distances. In addition, the deposition and zonal redistribution of dust may produce changes in the surface albedo and in the surface composition and thermal characteristics (Chrristensen, 1986).

Several authors have described or reviewed the topic of Martian dust storms (e.g., Gierasch, 1974; Zurek, 1982; Martin, 1984; James, 1985; Kahn et al., 1992;

* Paper presented at the *Seventh UN/ESA Workshop on Basic Space Science*, Tegucigalpa, Honduras, 16–20 June 1997.

Earth, Moon and Planets **77:** 19–46, 1997–1998.

Martin and Zurek, 1993; Zurek and Martin, 1993). Particular case studies have also been analysed and reported in the literature (e.g., Capen, 1974; Martin, 1974a,b, 1976; Briggs et al., 1979; Dollfus et al., 1984a,b).

The problem of Martian dust storms is posed by the question of what are the mechanisms controlling the origin, maintainence, and decay of the dust storms. This problem requires knowledge of the thermal structure and dynamical properties of the Martian lower atmosphere (e.g., Zurek et al., 1992).

In this article, different aspects of Martian dust storms will be described. These aspects include: classification of dust storms, properties of the airborne dust, seasonal and interannual variability of dust storms, their evolution, their causes, surface changes in atmospheric variables associated to Martian dust storms, models for these storms, and seasonal and long-term aspects of the dust cycle.

For the following discussion it is convenient to remember that the longitude of the Sun in Mars-centered (aerocentric) coordinates, L_s, is used as an angular measure of the Martian year with L_s 0°, 90°, 180°, and 270° marking the beginning of northern hemisphere spring, summer, fall, and winter (southern fall, winter, spring, and summer), respectively. A Mars solar day or sol is equal to 24.66 hours and a one Mars year is equal to 669.6 sols (or to 1.88 Earth years).

2. Classification of Dust Storms

Martin and Zurek (1993) compiled a comprehensive list of dust activity on Mars, from 1873 to 1990. They developed a classification scheme which takes into account the following aspects: (1) the size of the dust "event" (planet-encircling, regional, or local); (2) the nature of the identifying observations (e.g., photography, polarimetry, or spacecraft data); and (3) the type of activity (obscurations, stationary cloud, or storm). They did not attempted to include local dust storms observed by spacecraft, which were reviewed by Peterfreund (1981) and James (1985). Dust storms are dust clouds that were observed to move or expand (Zurek and Martin, 1993). The classification by size include: (a) the planet-encircling storm (a runaway storm that engulfs all longitudes, East-West, of Mars with dense clouds, although not necessarily simultaneously); (b) regional storm (long axis over 2000 km, but do not encircle the planet); and (c) local storm (long axis of affected area less than 2000 km). The planet-encircling storms have also been referred as "global" or "planetwide" storms. "Nonlocal" dust storms refers to both planet-encircling and regional dust storms (long axis over 2000 km), the obscuration of areas being greater than a few million square kilometers (Martin and Zurek, 1993; Zurek and Martin, 1993). Martin and Zurek (1993) feel that the terms "great" or "major" should be restricted to those events in either the encircling or the regional classes, thus excluding the "locals". Some images of dust storms are shown in Figures 1, 2, and 3.

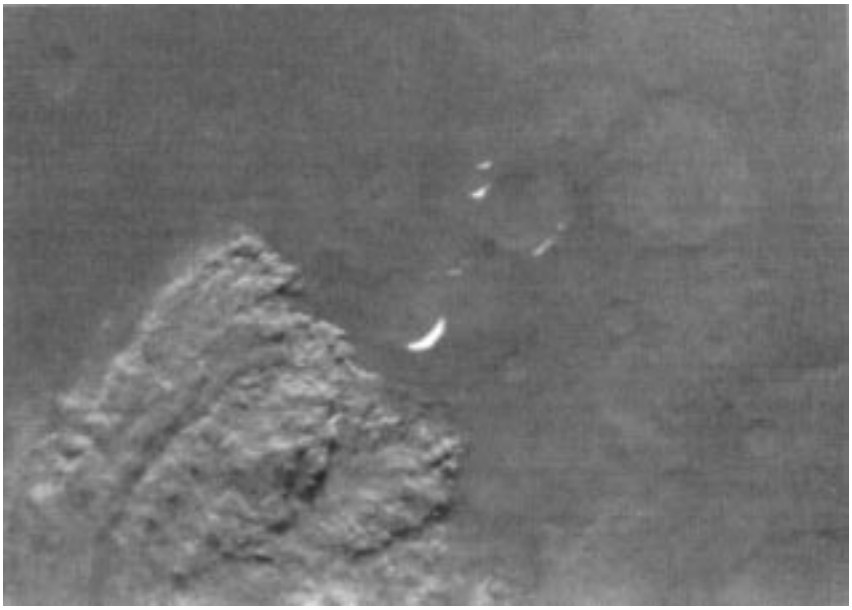

Figure 1. The end of a Mars global dust storm on the day after perihelion, at 3 pm local time (Viking Orbiter Image 248B57). The storm is near the edge of the shrinking south polar cap. This picture was taken by Viking Orbiter 2: the storm is about 200 km across, the frame width is 710 km, and the frame center is at 64 deg S. [Reproduced from "Weather, Climate and Life on Mars: Frequently asked questions answered-what causes dust storms?" (http://humbabe.arc.nasa.gov/mgcm/faq/dust.html), written and maintained by David Catling, Space Science Division, NASA Ames Research Center, with inputs from other scientists who study Mars including Bob Haberle, Jeff Hollingsworth, Mike Mellon, Jim Murphy, . . . so far.]

3. Properties of Airborne Dust

The intensity, scale and evolution of a dust storm are characterized mainly by the opacity (τ) of the dust. Zurek (1982) has described several attempts to estimate the opacity of the atmosphere under dust storm conditions. As pointed out by him, these attempts include studies which use: (a) Viking Lander images of the Sun and Phobos, (b) Orbiter TV images of the surface or the limb of the planet, (c) Orbiter infrared observations, and (d) less direct estimates using atmospheric temperature or surface pressure. Based on the works of Pollack et al. (1979) and Thorpe (1981), Zurek (1982) showed the visible (effective wavelength of 0.67 μm) optical depths, τ, of the dust haze above Viking Lander 1 (VL1) and Viking Lander 2 (VL2). He indicates the following: (1) the opacity increases sharply to large values ($\tau > 2$) at Lander 1 near L_s 205° and 279°, (2) the opacities at the two Lander sites (VL1 at 22.5°N, 48°W; VL2 at 48°N, 226°W) have similar trends but it is generally smaller at the more northern site, and (3) the opacity never seems to fall below a value of a few tenths at any time during the year. In addition, infrared optical depths estimates from the Viking Orbiter Infrared Thermal Mapper (Martin et al., 1979) and from

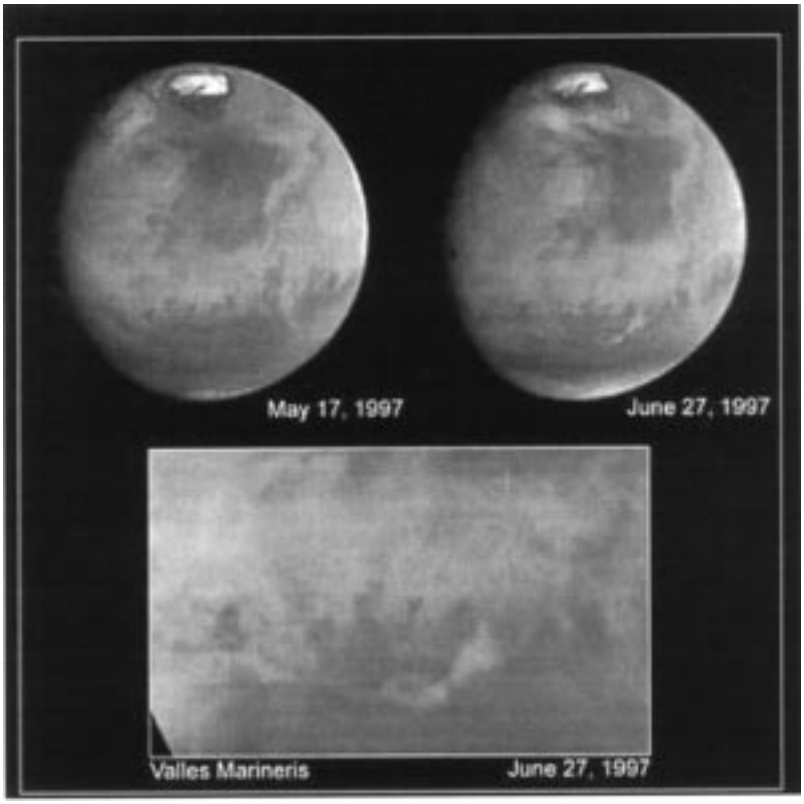

Figure 2. Top: These Hubble Space Telescope-WFPC2 images of Mars, taken on May 17 (left) and June 27 (right), 1997, reveal a significant dust storm which fills much of the Valles Marineris canyon system and extends into Xanthe Terra, about 1000 km south of the Pathfinder landing site. Visual comparison of these two images clearly shows the dust storm between 5 and 7 o'clock and about 2/3 of the way from the center to the southern edge of the June image. *Bottom:* The digital data were projected to form this map of the equatorial portion of the planet. The cross marks the approximate location of the pathfinder landing site, and the ribbon of dust which runs horizontally across the bottom of the map traces the location of Valles Marinaris. Most of the dust is confined within the canyons, which are up 5–8 km deep. The thickness of the dust near the eastern end of the storm is similar to that observed by Viking Lander 1 during the first two 1977 global dust storms which it studied. [Reproduced from "Canyon Dust Storm and Pathfinder Landing Site" (http://www.seds.org/hst/97-23.html), where other interesting features of these images are discussed. Credit: Steve Lee (University of Colorado), Mike Wolff and Phil James (University of Toledo) and NASA.]

the Lander surface pressure data (Zurek, 1981, 1982), indicate that the opacity of the dust haze above VL1 is fairly representative of the dust haze over low latitudes during the occurrence of great dust storms (large opacity). In the two major dust storms of 1977, the opacities at VL1 site remained elevated above the values prior to the storm for approximately 60 and 80 sols, respectively (Zurek and Martin, 1993).

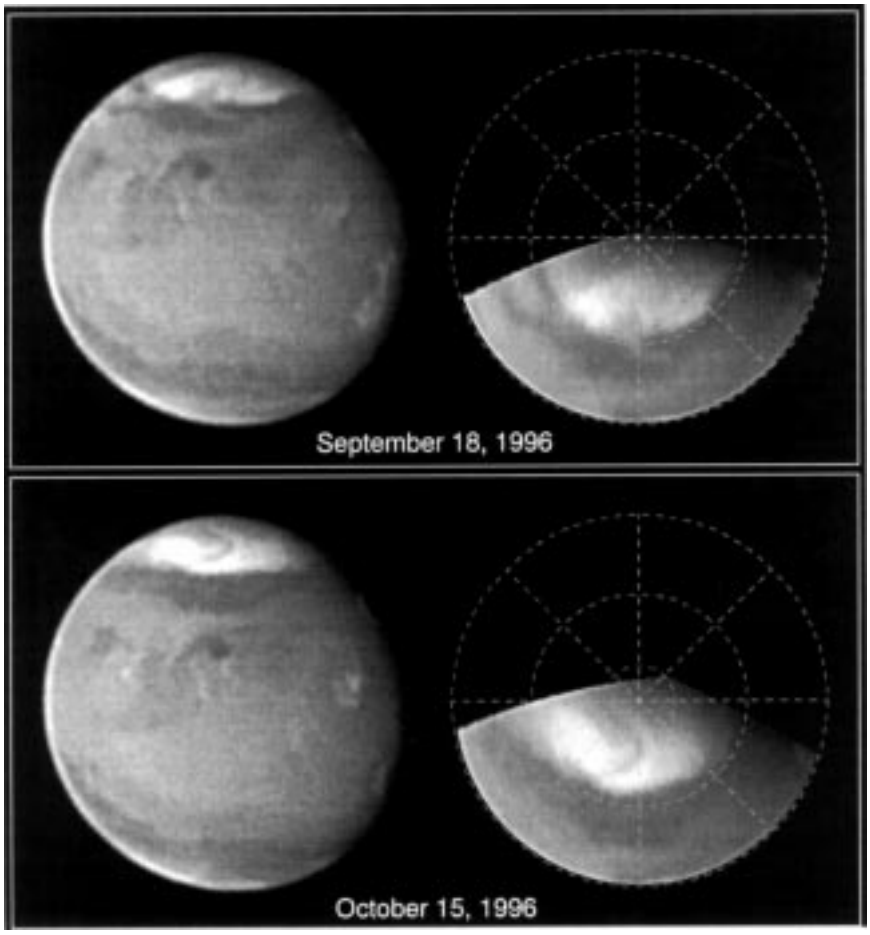

Figure 3. Two Hubble Space Telescope-WFPC2 images of Mars, taken about a month apart on September 18 and October 15, 1996, reveal a dust storm churning the edge of the Martian receding north polar cap. The images were assembled from separate exposures taken with the Wide Field Camera 2 (WFC2). *Top (September 18, 1996):* The notch in the white north polar cap is a 1000 km long storm. The bright dust can also be seen over the dark surface surrounding the cap, where it is caught up in the Martian jet stream and blown easterly. The clouds at lower latitudes are mostly associated with Martian volcanos such as Olympus Mons. *Bottom (October 15, 1996):* Though the storm has dissipated by October, a distinctive dust comma-shaped feature can be seen curving across the ice-cap. The shape is similar to cold fronts on Earth, which are associated with low pressure systems. To help compare locations and sizes of features map projections (right of each disk) are centered on the geographic north pole. Maps are oriented with 0 degrees longitude at the top and show meridians every 45 degrees of longitude (longitude increases clockwise); latitude circles are also shown for 40, 60, and 80 degrees north latitude. [Reproduced from "Springtime Dust Storm Swirls at Martian North Pole" (http://www.seds.org/hst/96-34.html). Credit: Phil James (University of Toledo), Steve Lee (University of Colorado) and NASA.]

Pollack et al. (1979) found from the Viking Lander data that visible optical depth had a value of about 1 just before the onset of each of the two major dust storms which occurred during the period of observations; it increased very rapidly on a time scale of a few days, to peak values of about 3 and 6 with the arrival of the first and second storm, respectively.

Clancy and Lee (1991), from an analysis of emission-phase-function (EPF) observations from the Viking Orbiter IRTM solar channel (passband = 0.3–3.0 μm, λ_{eff} = 0.67 μm), found that: (1) opacity ranges of 0.2–3.0 with a L_s dependence similar to the Viking Lander results (Pollack et al., 1979); (2) dust opacities as high as 0.4 at the summit of Olympus Mons, and as high as 0.8 near the south pole during the global dust storm of 1977; (3) a dust scattering phase function identical to that derived from the Viking Lander observations, but the single scattering asymmetry parameter in both cases is 0.55–0.56 rather than 0.79; (4) a dust single scattering albedo of 0.92, as compared to the Viking Lander result of 0.86; (5) dust particle sizes may be 5–10 times smaller than suggested by Toon et al. (1977), based on the Viking Lander visible scattering phase functions and the observed ratio of visible and infrared dust opacities.

Recently, Ockert-Bell et al. (1997) developed a wavelength model of the single scattering properties of the Martian dust using the particle size distribution, shape, and single scattering properties at Viking Lander wavelengths given by Pollack et al. (1995). They have listed the values (as function of wavelength) of the dust single scattering albedo (ω_0), single scattering asymmetry parameter (g), extinction factor (Q_{ext}), real index of refraction (n_r) and complex index of refraction (n_i) in the 0.21–4.15 μm wavelength range. For the wavelength of 0.67 μm, the values of ω_0,g, Q_{ext}, n_r, and n_i are 0.93, 0.65, 3.04, 1.51, and 0.003, respectively. Their values of ω_0 in the 0.21-1.015 μm wavelength range, which vary from 0.72 to 0.95, were modified by Wolf et al. (1997) in the blue/ultraviolet and at 1.015 μm to provide consistent fits of the Hubble Space Telescope data to derive cloud opacity.

The thermal infrared (9 μm) opacity of dust has been derived from brightness temperature measurements made by the Viking Orbiter Infrared Thermal Mapper (IRTM) data (e.g., Martin et al., 1979; Hunt et al., 1980; Martin, 1986; Martin and Richardson, 1993). The infrared spectral measurements are very sensitive to the presence of dust, which has a strong absorption band at 9 μm (e.g., Hunt et al., 1980). Since the extinction factors at the visible and infrared wavelengths are affected by both the composition and the particle size distribution, the ratio between the Lander (visible) and infrared (9 μm) opacities gives information about the nature of the dust (Martin, 1986). For comparison with the Lander opacities, the infrared opacities are scaled by some factor. A value of 2.5 for the visible-to-infrared ratio of opacity fits the results obtained by Martin (1986) and Martin and Richardson (1993). Zurek (1982) found values for such a ratio of 1.85 using the derived infrared opacities of Martin et al. (1979), and of 1.2 for montmorillonite and the size distribution of Pollack et al. (1979). A value of 1.69 for the visible-to-infrared ratio of opacity was used by Hunt et al. (1980) to derive the visible

opacity from the infrared opacity. Hunt et al. (1980) found values of 9 μm opacity of about 2.5 in the most opaque regions of a local dust storm. Several kilometers away from the center, the atmosphere was still very dusty, with infrared opacity up to approximately 1.4. Correspondingly, the visible opacity is in the 2–5 range.

The use of Viking IRTM data for opacity derivation is important for mapping purposes (Hunt et al., 1980; Martin, 1986; Martin and Richardson, 1993). The coverage of the IRTM data is greater than that of the imaging experiment. A global dust opacity mapping for Mars was performed by Martin and Richardson (1993) from Viking IRTM data. The period considered is from the beginning of Viking observations until L_s 210° in 1979 (1.36 Mars years). This allowed the authors to study the evolution of the two major dust storms of 1977. In addition, their 9 μm opacity maps have been used by Martin (1995) to make estimates of the mass of dust suspended in the Martian atmosphere. He found that the maximum dust content during the 1977b storm amounted to about 4.3×10^{14} g, which corresponds to about 4.3×10^{-4} g/cm^2, or a layer 1.4 μm thick, if densely compacted. He also found that during a local dust storm near Solis Planum at L_s 227°, about 1.3×10^{13} g of dust were lofted.

Some evidence has been found that the dust particles are nonspherical, which has important optical effects at visible and shorter wavelengths (Thorpe, 1978; Pollack et al., 1977, 1979). As pointed out by Clancy et al. (1991), the generally accepted model of the dust particle size distribution is based on the analyses of Mariner 9 Infrared Interferometer Spectrometer (IRIS) spectra of dust and on the Viking Lander observations of the visible scattering phase function of atmospheric dust (Toon et al., 1977). The distribution is a modified gamma distribution with a mode radius of 0.4 μm and an average cross-section weighted particle radius (r_{eff}) of 2.5 μm. Other particle size distributions, in which r_{eff} is smaller than 2.5 μm, have been deduced or used by other researchers (e.g., Drossart et al., 1991; Clancy et al., 1995; Pollack et al., 1995); see also Table I. For example, Pollack et al. (1995) used a lognormal particle size distribution with r_{eff} = 1.85 μm, whereas Smith et al. (1997) using Pathfinder's data estimated r_{eff} to be 1.0 (+0.3, −0.2) μm. Results by Clancy and Lee (1991) indicate that the Viking Lander observations are at least consistent with r_{eff} = 0.4 μm. This is in agreement with the results of Pollack et al. (1977). Several arguments given by Clancy and Lee (1991) provide evidence that dust in the Martian atmosphere is composed of very fine particle sizes ($r_{\text{eff}} \leq 0.4$ μm).

With regard to composition of dust, magnetite has been identified as a particle mineral (Pollack et al., 1979), as well as mixtures of montmorillonite and basalt (Toon et al., 1977). Hanel et al. (1972) found that dust particles have a composition that corresponds approximately to that of rocks of intermediate SiO_2 content. Clancy et al. (1995) found that a much broader, smaller particle size distribution coupled with a "palagonite-like" dust composition fits the complete ultraviolet-to-30 μm absorption properties of the dust better than the distribution and mixture of montmorillonite and basalt dust composition given by Toon et al. (1977).

TABLE I

Compilation of martian dust particle properties inferred from spacecraft observations (from Murphy et al., 1993)

λ, μm	Mean radius, μm	Other parameters	Comments	Source
Ultraviolet				
0.263, 0.300	2	r decrease with time; opacity decreases from 1 to 0.05	South pole; the number of larger particles decreases with time	Mariner 9; Pang and Hord (1973)
0.268, 0.305	1	Variance ∼0.4	Composition is not dominated by montmorillonite	Mariner 9; Pang et al. (1976)
0.268, 0.305	0.2	Nonspherical particle shape	Nonspherical shape effects allow for montmorillonite	Mariner 9; Chylek and Grams (1978)
Visible				
0.585	10	$\omega_0 \sim 0.7 - -0.85$	Surface particles are of similar size	Mariner 9; Leovy et al. (1972)
0.565, 0.610	2.5, 5.0	Smaller particles at higher altitudes	From clarity of surface features at various surface elevations	Mariner 9; Hartmann and Price (1974)
0.67	0.4	Nonspherical	2 northern hemisphere sites only	Viking Lander; Pollack et al. (1977)
0.67	2.5	r_m = 0.4 μm, ω_0 = 0.86, γ=0.79; **nonspherical shape**	2 northern hemisphere sites only	Viking Lander; Pollack et al. (1979)
0.493, 0.592	–	$\omega_0 \sim 0.5$; λ = 0.592 μm $\omega_0 \sim 0.8$; λ = 0.443 μm, $g < 0.6$	Global perspective	Viking Orbiter; Thorpe (1978, 1981)
0.592	–	$g \sim 0.55$–0.66, $\omega_0 \sim 0.9$–0.98	Planet limb viewing	Viking Orbiter; Jaquin et al. (1986)
0.3–3.0	0.4	$\omega_0 \sim 0.92$, $g \sim 0.55$	Little variation with space or time	Viking Orbiter EPF; Clancy and Lee (1991)

TABLE I
Continued

λ, μm	Mean radius, μm	Other parameters	Comments	Source
Infrared				
5–50	1–10	–	Based upon comparisons with synthetic spectra	Mariner 9 IRIS; Conrath et al. (1973)
0.7, 1.38	0.5–1	–	Dust-induced "anti-greenhouse" effect	Mars 2 and 3; Moroz and Ksanfomaliti (1972)
15	1	–	Based on particle sedimentation lifetimes	Mariner 9; Conrath (1975)
5–50	2.5	r_m = 0.4μm, modified gamma distribution	Size distribution is constant at subsolar latitudes	Mariner 9 IRIS; Toon et al. (1977)
7–45	–	–	Fewer large particles at south pole than at lower latitudes	Mariner 9 IRIS; Paige et al. (1987)
7, 9, 15, 20	-	–	Derived 9-μm opacities are a factor of 2.5 less than observed values	Viking IRTM; Martin (1986)
–	–	–	Apparent "neutral" greenhouse effect due to dust	Viking Lander; Haberle and Jakosky (1991)
5–50	–	$r_m \sim 0.5\ \mu$m, variance ~0.15	Post-1971–1972 dust storm; palagonite is a representative mineral	Mariner 9 IRIS, Santee and Crisp (1991)

λ represents the wavelength(s) employed in the various studies listed.

Murphy et al. (1993) made a compilation of Martian dust particle properties inferred from spacecraft observations (see Table I). Other useful information about properties of airborne dust on Mars has been provided by Kahn et al. (1992).

Profiling of Mars atmospheric temperature has been obtained from Earth-based microwave measurements of 1.3 mm and 2.6 mm rotational spectra of Mars atmospheric CO (Clancy et al., 1990, 1994, 1996). The disk-average (i.e., low- to mid-latitude) atmospheric temperatures obtained with this technique as early as 1975 allow determination of dust storms, because if the atmosphere has a larger amount of dust it is generally warmer and more isothermal than a relatively clear atmosphere. Abrupt increases of Mars atmospheric temperature at the 0.5 hPa level (greater than 20 K), obtained from the microwave CO spectra in 1992 (L_s 228°) and 1994 (L_s 254–283°), compare favorably with the temperature increases at the 0.5 hPa level obtained by Viking IRTM at the beginning of the two 1977 global dust storms (Clancy et al., 1996). The occurrence of two global dust storms, one in 1992 (Clancy et al., 1996) and another in 1994 (Clancy et al., 1994, 1996), was inferred from these observations. As pointed out by Clancy et al. (1996) neither of the 1992 and 1994 microwave identifications of Martian global dust storms have been verified by Earth-based imaging. Clancy et al. (1996) have indicated that this lack of supporting Earth-based measurements is due to the difficulty of observing Mars around conjunction, which coincides with the so called dust storm season during the last two cycles. For this reason, the 1977 Mars global dust storms were not observed from Earth-based imaging. Microwave observations of CO emission lines from the Mars atmosphere will greatly augment our knowledge of interannual variability of dust storms.

4. Seasonal Variability of Dust Storms

Martin and Zurek (1993) found that dust storms have originated in many different regions of Mars. In general, for all size classifications, there is more activity in the southern hemisphere and in specific regions like Hellas (light albedo).

All planet-encircling storms have been observed during the southern spring and summer seasons, although there is significant interannual variability. These storms began between L_s 204° and 310°, during the south polar cap recession (Martin and Zurek, 1993). The initial clouds for planet-encircling storms have occurred over dark areas. In most cases this initial area has been Hellespontus (dark albedo).

Regional dust storms occur in nearly all seasons, with the two principal exceptions being L_s 130°–160° and 330°–20°, and they occur more frequently than planet-encircling storms (Martin and Zurek, 1993). They do tend to occur most frequently (L_s 160°–330°) during the southern spring and summer seasons, in the so called “dust storm season”.

The period L_s 161°–326° has been referred to as “dust storm season” (Martin and Zurek, 1993). This period is nearly centered on perihelion (L_s 250°), which

is the time of maximum insolation on Mars. This enhance atmospheric convection during daytime, as well as thermal circulations induced by topography.

So, both seasonal ranges (for planet-encircling and regional dust storms) are somewhat centered on perihelion.

5. Interannual Variability of Dust Storms

Martin and Zurek (1993) found that there is significant interannual variability in the occurrence of planet-encircling dust storms. In addition, Zurek and Martin (1993) found that "the chance of a planet-encircling dust storm occurring in any arbitrary Mars year is estimated to be approximately one in three (18–55% at the 95% level of confidence), if such occurrence is random from year-to-year and yet restricted seasonally to southern spring and summer". So, as they do not occur every Martian year, it appears that seasonal conditions in themselves do not provide the requirements for smaller storms to evolve into planet-encircling storms. Thus, as pointed out by Martin and Zurek (1993), "we must go beyond the question of how to raise dust, to how do a few dust storms perpetuate themselves but other do not?".

The probability for nonlocal dust storms to occur during a given storm season is approximately 80%, reflecting the large number of detections of regional, but not planet-encircling dust storms (Zurek and Martin, 1993).

Ingersoll and Lyons (1993) proposed the hypothesis that the global Martian climatic system, consisting of atmospheric dust interacting with the atmospheric circulation, produces its own interannual variability when forced at the annual frequency. This is supported by their findings in which the interannual variability manifests itself either as a periodic solution in which the period is a multiple of the Martian year, or as an aperiodic (chaotic) solution that never repeats.

6. Evolution of the Dust Storms

There are only five well-documented cases of planet-encircling dust storms, which occurred in 1956, 1971, 1973, and 1977 (two). However, as pointed out before, Earth-based microwave measurements of Mars atmosphere have provided evidence of the occurrence of global dust storms in 1992 and 1994 (Clancy et al., 1994, 1996). Ebisawa and Dollfus (1986) found that in 1956, 1971, and 1982, the planet-encircling dust storms manifested sharp-cut boundaries (did not display irregular or diffuse outlines) at their outbreak in the early stage of their evolution. They have also pointed out that the dust is first raised in specific and precisely localized regions and at this stage it does not spread out quickly. Actually, these local dust clouds (bright spots in Earth-based photography) expand slowly during this initial phase, which last usually less than a week. In the next several days, new dust clouds develop and old ones merge, the dust cloud expands and moves toward other

regions; its outlines are irregular and diffuse. Secondary local dust clouds may develop at new locations. The planet-encircling dust storms expand first zonally (east-west direction) until a latitudinal band is obscured, which is followed by a expansion in the north-south direction (Martin, 1974a,b, 1976). Their minimum lifetime is 3 or 4 weeks, while regional storms probably do not last more than 2 weeks (Martin, 1984). It was found that the planet-encircling dust storm of 1971 went through a daily cycle of regeneration, although each day it advanced farther than it did the day before (Martin, 1974a).

There are only two known regions in which planet-encircling storms originate: Helles-Hellespontis and Solis Planum-Claritas Fossae (Martin, 1984). The areas subject to local and regional dust activity are much more numerous and have been mapped by Martin and Zurek (1993).

7. Causes for Dust Storms

7.1. THE SALTATION MECHANISM

In order for a dust storm to be formed, dust particles must be rised into the atmosphere, possibly by the saltation mechanism (Bagnold, 1941). The surface characteristics and the boundary layer flow are also involved in the process of rising dust into the atmosphere. The extension of Bagnold's work to Martian conditions has been carried out by several authors (e.g., Gifford, 1964; Ryan, 1964; Sagan and Pollack, 1967; Hess, 1973) and has been summarized by Gierasch and Goody (1973). Assuming that the drag coefficient (C_d) of a sand grain is a function only of the particle Reynolds number, the minimum friction velocity to raise sand ($U^*_{\min}$) is given by:

$$(U^*_{\min})^3 = \text{constant}(\sigma g \nu/\rho), \tag{1}$$

where σ is the grain density,g is gravity acceleration, ν kinetic viscosity, ρ air density, and the constant is 1.2×10^2 from Bagnold's data. For CO_2 at 200 K and 6 hPa, Gierasch and Goody (1973) found that $U^*_{\min}$ = 180 cm s^{-1}, as compared to 15 cm s^{-1} for terrestrial conditions. According to Csanady (1967), the friction velocity (U^*) relates to the approximately geostrophic free-steam velocity (U_g) as follows:

$$(U^*/U_g)^2 = C_d, \tag{2}$$

where C_d is the drag coefficient. Leovy and Mintz (1969) used the following relationships:

$$U^* = 3 \times 10^{-2} U_g, \quad \text{for stable conditions} \tag{3a}$$

$$U^* = 6 \times 10^{-2} U_g, \quad \text{for unstable conditions.} \tag{3b}$$

For unstable conditions on Mars, with $U^* = 180$ cm s^{-1}, $U_g = 30$ m s^{-1}. Iversen et al. (1976a,b) obtained a threshold friction velocity for Mars of about 2 m s^{-1}.

The particles which are most likely to be moved at the ground have an approximated radius of 100 μm (Greeley et al., 1980). Saltation of particles of this size will cause the raise of smaller particles from the ground, some of which will return to the surface because of setting. Wind speeds larger than 25 m s^{-1} at 1.6 m above the ground were recorded by VL1 during a local dust storm (Ryan et al., 1981; James and Evans, 1981). Moore (1985) pointed out that, during the Martian dust storm of sol 1742 at VL1, winds probably attained speeds of about 40–50 m s^{-1} at a height of 1.6 m above the surface and friction speeds were probably about 2.2–4.0 m s^{-1}; a spectrum of particle sizes from ten or so micrometers and clods, up to 4–5 mm, were salted by and entrained in the wind. A comprehensive discussion of the mechanisms by which dust may be transported from the surface into the atmosphere (which is beyond the purpose of this article) is given by Greeley et al. (1992).

Properties of surface particulate materials have been determined from thermal inertia data obtained from the Mars Gobal Surveyor thermal emission spectrometer, the Viking IRTM, and the Mariner 9 infrared radiometer (e.g., Kieffer et al., 1973; Edgett and Christensen, 1991; Presley and Christensen, 1997b). For example, Edgett and Christensen (1991) found that thermal inertia data indicate that Martian aeolian dunes have an average particle size of about 500 $\pm$ 100 μm. They also found that the particle size transition from suspension to saltation is about 210 μm. These results are consistent with particle sizes of 400–460 μm for 270 IU as derived by Presley and Christensen (1997b). A review of the methodology available for the study of thermal conductivity of particulate materials – with emphasis on low atmospheric pressures – is given by Presley and Christensen (1997a). Experiments carried out by Presley and Christensen (1997b) have shown that thermal conductivity is approximately related to particle diameter and atmospheric pressure (in the 1–100 torr range) by the relation:

$$\kappa = (C P^{0.6}) d^{-0.11 \log(P/K)}, \tag{4}$$

where κ is the thermal conductivity in W/(m K), P is atmospheric pressure in torr, d is the particle diameter in μm, $C \approx 0.0015$, and $K \approx 8.1 \times 10^4$ torr (when these units are used). This relation is valid for particulate materials that have a medium well-packed bulk density (Presley and Christensen, 1997b). The particle size dependence of the thermal conductivity derived by Presley and Christensen (1997b) is significantly different from the estimate by Kieffer et al. (1973), except for 200 μm particles. Presley and Christensen (1997c) found that particle shape influences the thermal conductivity primarily by affecting the bulk density and that significant differences in bulk density influence the thermal conductivity.

7.2. POLAR CAP RECESSIONS AND MAJOR DUST STORMS

Most of the dust events (78%) studied by Martin and Zurek (1993) occurred between L_s 161° and 326°, during the recession of the south polar cap. However, no events were observed during the two periods when the contracting caps are close to their minimum size, and sublimation has become minimal. Therefore, it appears that there is some relationship between polar cap recessions and major dust events and that possibility might be strongest for the south polar cap. This is supported by the Viking images, which show local dust near the edges of the receeding caps (Briggs et al., 1979). The relationship between polar cap recessions and dust storms is the result of strong local and large-scale winds due to large temperature gradients at the polar cap edge and mass outflow of the subliming cap (Leovy et al., 1973; Burk, 1976; French and Gierasch, 1979; Haberle, 1979; Haberle et al., 1979; Fernández, 1995a,b). Besides this situation, the regions where major dust storm develop show favorable topographic characteristics: slopes and uplands which can enhance atmospheric convection and flow lifting by orography, as well as particular surficial properties (e.g., albedo and thermal inertia). A study of the Martian boundary layer, taking into account topography, was made by Blumsack et al. (1973). They found, 1 km above a Martian slope of 0.005, variations in the temperature of $\pm$ 15 K and in the upslope wind of $\pm$ 25 m s^{-1}. Magalhaes and Gierasch (1982) have also studied wind induced by slopes on Mars. They found that for a surface with low thermal inertia and large roughness length wind speeds in the early morning hours can produce saltation. Some preliminary studies about the effects of topography on baroclinic instability were made by Blumsack and Gierasch (1972).

7.3. THE POLAR CAP BREEZE

The line of separation between the Martian polar caps and the "desert" (frost-free) adjacent areas constitutes a discontinuity in meteorological boundary conditions. The polar caps are composed of CO_2 while the "desert" areas are formed mainly by dust particles with a composition that corresponds approximately to that of rocks of intermediate SiO_2 content (Hanel et al., 1972). The difference in the response capabilities of the polar cap and the "desert" areas to the radiation field originates a meridional temperature gradient, which produces in the atmosphere a baroclinic instability. This generates an atmospheric circulation system similar in some aspects to the terrestrial sea breeze. Fernández (1995a,b) called this circulation system the Martian polar cap breeze.

From calculations made by Pallmann and Frisella (1972, Fig. 5) and by Pallmann et al. (1973, Fig. 13), it can be seen that in summer time the smallest temperature difference between the polar cap and the "desert" adjacent areas occurs at about 04:00 local time and has a value of about 74 K. The greatest temperature difference occurs near 15:00 local time and is then about 102 K. The surface temperature of the polar cap is the frost point temperature of CO_2 (148 K) and

it is an equilibrium temperature of the solid and gaseous phases. Since the "desert" areas are much warmer than the polar cap, and being that density decreases upward, the surfaces of constant density slope upward from the "desert" areas to the polar cap. Because the isobaric surfaces are usually more nearly horizontal, the two sets of lines intersect to form a solenoid field in the vertical plane (baroclinic effect). If we assume for a moment that Mars is a longitudinally uniform nonrotating planet and if we ignore friction, then the solenoid field originates a circulation system consisting of a desertward current adjacent to the surface, and a much weaker return above. The baroclinic effect would cause progressively increasing wind speeds. In addition to the Coriolis and friction effects, other factors influence the polar cap breeze (Fernández, 1995a). They are: the prevailing wind, topography, irregularity of the polar cap-edge, stability of the atmosphere, and seasonal variations.

Burk (1976) and Fernández (1995b) have made numerical simulations of the polar cap breeze, utilizing models constructed in part from work previously done by others on the terrestrial sea breeze. For a situation in which the cap edge was taken to be at 65°S, Burk (1976) found maximum horizontal winds of approximately 20 m s^{-1} when the early morning temperature profile was isothermal. Fernández (1995b) found maximum wind speeds of about 15 m s^{-1} when the polar cap is near 50°S and based on the data given by the Mariner 6 exit, which presented an inversion of $\gamma = -3.3$ K/km near the ground. Although these winds are not strong enough to rise dust, they may act together with other wind regimes.

It should be pointed out that these simulations did not considered several effects that influence the polar cap breeze and which may produce stronger winds, such as thermal and mechanical circulations induced by topography.

7.4. THE LARGE-SCALE POLAR CAP WIND

The polar cap breeze is a local wind phenomenon affecting only the immediate vicinity of the polar cap-edge. There is also a large-scale polar cap-and-"desert" wind thermally induced by the general temperature differences between the two areas. Leovy and Mintz (1969) made calculations of meridional and zonal winds for two experiments; one simulates orbital conditions at the southern summer (northern winter) solstice of Mars, and the other, orbital conditions at the southern autumnal equinox. At the solstice, the mean meridional circulation shows intense thermally directed circulation: the air rising in the subtropics of the summer hemisphere, moving northward at the upper level, and descending in the winter subtropics. There is some indication of a weaker reverse cell at high latitudes (approximately 30°). However, the winds are extremely light. In the southern autumnal equinox experiment, the meridional winds are much weaker.

Haberle et al. (1993) have made numerical simulations of Mars atmospheric general circulation with the NASA Ames General Circulation Model. At the southern summer (northern winter) solstice and when the atmosphere is relatively clear they found that the mean meridional circulation consists of three cells: a large and

intense cross-equatorial Hadley cell with rising and descending branches centered at 30°S and 30°N, respectively; a thermally indirect Ferrel cell at high northern latitudes, and a weak Hadley cell – with lower level horizontal winds from polar cap to "desert" areas – at high southern latitudes. They also found that over 75% of the mass supplied to the rising branch of the cross-equatorial Hadley cell flows through the lowest several kilometers of the atmosphere and that the mean meridional motions are about a factor of 6 stronger on Mars than on Earth. At the southern winter solstice, the cross-equatorial Hadley circulation (with its rising branch at northern mid-latitudes) is considerably weaker compared to northern winter. A Hadley cell at high southern latitudes is also present at the southern winter solstice, but the horizontal flow at lower levels is toward the pole. In the equinox experiments, the cross-equatorial Hadley cell almost disappears and there are two Hadley cells of comparable strength, one over the Southern Hemisphere and the other over the Northern Hemisphere. In the Southern Hemisphere, large-scale wind at lower levels from polar cap to "desert" areas is observed in the spring and fall equinox experiments (Haberle et al., 1993).

A numerical study of the large-scale polar cap winds on Mars was carried out by Haberle et al. (1979). Their approach consisted of utilizing the complete nonlinear equations in sigma-coordinates to determine the seasonal variation of the middle and high latitude circulation system. The spacing between grid points was 2.5 (148 km) and lateral boundaries were set at 27.5°N and 90°N. They considered the following factors: seasonal thermal forcing, mass exchange between polar caps and atmosphere, large-scale topography, and polar cap size. During spring, the thermal forcing sets up a circulation with easterlies equatorward of the cap-edge and easterlies poleward of it; the maximum westerlies occur where the horizontal temperature gradients are largest. Vertical motions are strongest in the vicinity of the polar cap-edge with rising motion over the "desert" areas and sinking motion over the polar cap. The intensity of the circulation is proportional to the cooling power or size of the polar cap. This pattern changes for other times of the year. In winter, surface winds are westerly over the entire cap and part of the adjacent "desert" areas. In late winter and early spring, a two-cell circulation is observed with an inflow at the higher latitudes of the polar cap and an outflow at the lower latitudes. Their results also show that surface winds near the edge of a retreating polar cap are significantly enhanced. The maximum surface winds are 20 m s^{-1} during spring and 30 m s^{-1} during winter for the Northern Hemisphere.

7.5. ATMOSPHERIC TIDES AND DUST STORMS

On the planetary scale, as pointed out by Zurek (1982), diurnal variation of surface heating during relatively clear periods and of solar heating of the airborne dust during dusty periods drives large-amplitude atmospheric tides, with the tidal winds having their near surface maximum speeds 20° of latitude away from equator. This may be the explanation for the tendency of local dust storms to form in the

subtropics of both hemispheres. Leovy and Zurek (1979) found, from observations of surface pressure oscillations at VL1 and VL2 sites that the thermally driven global atmospheric tides were closely coupled to the dust content of the Martian atmosphere.

7.6. MID-LATITUDE SYNOPTIC WEATHER SYSTEMS

Cold fronts associated with mid-latitude baroclinic waves have been proposed as a mechanism for the generation of local dust storms, observed particularly in northern hemisphere mid-latitudes during fall and winter (Leovy et al., 1972; Tillman et al., 1979; Ryan et al., 1981; James, 1985). The wind speeds may be increased by other factors (James and Evans, 1981). This mechanism is responsible for the generation of a large number of terrestrial dust storms in mid-latitudes in winter (James, 1985). Baroclinic waves could be an important factor not only in the generation of local dust storms but also in the growth and development of larger dust storms (Ryan and Sharman, 1981). Fronts were frequently observed at the VL2 site during fall and winter (Tillman et al., 1979). The passage of eastward travelling baroclinic waves with centers north of the VL2 site has been analysed from surface observations by Ryan et al. (1978) and Ryan and Sharman (1981). These surface observations are described in the next section. The joint action of a baroclinic wave and the diurnal thermal tide (when combined in phase) may produce strong winds (Ryan and Sharman, 1981; James, 1985). Transient baroclinic eddy activity has been studied from General Circulation Model (GCM) simulations by Barnes et al. (1993). They found a strong transient baroclinic eddy activity in the extratropics of the northern hemisphere during the northern autumn, winter, and spring seasons. The simulated eastward propagating eddies are characterized by zonal wavenumbers of 1–4 and periods of 2–10 days. In addition, Barnes et al. found a very weak transient baroclinic eddy activity in their southern winter simulations. According to them, it appears that this is partly a consequence of the stabilizing effects of the zonally symmetric topography in the GCM, but it also must be associated with certain aspects of the zonal-mean circulation in the southern winter.

7.7. DUST LOAD PRIOR TO THE ONSET OF DUST STORMS

Observations suggest that the Martian atmosphere had a great amount of dust load just prior to at least some of the planet-encircling dust storms (Pollack et al., 1979; Martin et al., 1991a). This indicates that a dusty atmosphere may provide favorable conditions for the development of these storms (Leovy et al., 1973; Leovy and Zurek, 1979; Harberle et al., 1982; Martin et al., 1991b).

8. Surfaces Changes in Atmospheric Variables

Ryan and Henry (1979) and Ryan and Sharman (1981) studied surface changes in meteorological variables at VL1 (22.5°N, 48°W) and VL2 (48°N, 230°W) associated with the arrival of major dust storms. The arrivals of the storms were accompanied by significant increase in wind speed and pressure at VL1; no such changes were observed at VL2. A decrease in temperature range (due to a decrease in maximum temperature and an increase in minimum temperature) was observed at both sites. According to Ryan and Henry (1979) the wind directions during the period of increase on sol 209 followed the same diurnal pattern as on previous sols, switching from westerlies to easterlies in early afternoon, implying an intensification of the tidal pattern rather than a response to a synoptic pressure system. Ryan and Sharman (1981) have pointed out that the increase in diurnal pressure amplitude is caused by increases in the tides as well as baroclinic waves. The semidiurnal tide in particular is the basis indicator of "global" dust content. Ryan and Sharman (1981) have also pointed out that a pressure periodicity of 2–3 sols is evident and that the wind vector exhibits clockwise rotation in synchronization with the pressure waves. This is due apparently to the passage of eastward traveling baroclinic waves with centers north of the VL2 site (Ryan et al., 1978). From general circulation model (GCM) runs, Pollack et al. (1993) found that atmospheric dynamics have a significant impact on the seasonal pressure variations measured at VL1 and VL2 sites.

9. Models for Dust Storms

As pointed out by Zurek (1982), any model attempting to explain the origin of the great dust storms must address at least three critical questions: (1) why do these precursor storms originate only in certain areas during certain seasons, (2) by what mechanism do some, but certainly not all, local storms evolve to planetary scale, and (3) how widespread is the source of the dust that eventually winds up in the planetary-scale dust haze? A fourth question (also pointed out by Zurek, 1982) is: where is the dust raised by a great dust storm deposited?

Several mechanisms have been proposed for the generation of major dust storms. They may be divided in two classes (Gierasch, 1974; Zurek, 1982) based on the enhancement of: (1) the planetary-scale components of the atmospheric circulation (e.g., Leovy et al., 1973; Houben, 1982), and (2) small but expanding vortical motion through a strong dust feedback (e.g., Gierasch and Goody, 1973; Golitsyn, 1973; Hess, 1973).

9.1. MECHANISMS RELATED WITH LARGE-SCALE ATMOSPHERIC CIRCULATION

These mechanisms may be summarized as follows (Leovy et al., 1973). During southern spring local dust storms develop in the baroclinic zone adjacent to the contracting south polar cap. This zone is characterized by strong local and large-scale winds produced by large temperature gradients and sublimation of the polar cap. These winds, enhanced by topographic characteristics (sloping terrain and uplands), rise the dust forming local dust storms in preferred areas such as Hellas and Argyre. These local storms generate and dissipate during a period of several days. The diabatic heating due to absorption of solar radiation by the dust intensifies the general circulation, mainly over sloping terrain in the 20–40° latitude band, which in turn maintain the formation of local dust storms that eventually merge and develop into a major dust storm. The upper-level northward flow is also intensified and the dust moves toward equator (to lower latitudes). As the dust rises in the ascending branch of the cross-equatorial solsticial circulation it spread faster due to vertical wind shear (wind increasing with height).

The northward expansion of the storms depends of how high the dust is raised. Harbele et al. (1982) found, using a numerical model, that dust must raise up to 20 km in order to significant northward transport may occur. Other studies (Leovy et al., 1972; Conrath et al., 1973) show that during planet-encircling dust storms the dust was present in the 40–60 km altitude range.

The decay phase of the dust storms is the result of increasing static stability over the regions where dust is rised (Leovy and Zurek, 1979; Pollack et al., 1979) and the suppression of surface heating when opacities are greater than one (Pollack et al., 1979). The decay phase may last approximately between 50 and 75 sols (e.g., Zurek, 1982).

Leovy et al. (1973) used a numerical model to simulate the characteristics of three components of the global wind system during the planet-encircling dust storm of 1971. These three components of the wind system are the steady axially symmetric component, and the diurnal and semi-diurnal tides. They found that zonally averaged surface wind speeds in the equatorial zone were near 30 m s^{-1}, which are strong enough to rise dust by saltation (Golitsyn, 1973; Gierasch and Goody, 1973). The pattern of these winds corresponds well with the pattern of observed light surface streaks (light albedo markings trailing from craters and other topographic features). These streaks extend from northeast to southwest in the northern tropics and from northwest to southeast in the southern tropics (Sagan et al., 1973). Leovy et al. (1973) also found that the surface winds due to the diurnal and semidiurnal tides were not strong enough to rise dust, although they contribute significantly to the total wind. The factors responsible for the intensification of meridional circulation are strong insolation, low static stability, and high atmospheric absorptivity and emissivity (Leovy et al., 1973).

The effects of dust on the thermal structure and the dynamics of the Martian atmosphere have been studied by several investigators (e.g., Gierasch and Goody, 1972; Haberle et al., 1982; Schneider, 1983; Pollack et al., 1979, 1990; Murphy et al., 1990, 1993; Santee and Crisp, 1993). Some results are summarized below.

Haberle et al. (1982) used a primitive equation model to study the transport of dust away from a southern surface source at L_s 270°, as well as the changes due to the absorption of solar and infrared radiation by dust and CO_2. Their results show that dust is very effectively transported by the zonal mean circulation which rapidly increase in intensity and spatial extent as the dust spreads.

Schneider (1983) used a steady, zonally symmetric, nearly inviscid model to study the development of planet-encircling dust storms. His results indicate that as the heating is increased from zero, some critical value is reached at which the response jumps from local to global, which may be related to the observed "explosive" growth of planet-encircling dust storms.

Murphy et al. (1990) made numerical simulations of the decay of Martian planet-encircling storms, using an aerosol transport/microphysical model. They found that temporal and spatial variations of the size distributions of the particles suspended in the atmosphere are important factors of the decay of dust storms.

Murphy et al. (1993) studied the size-dependent transport of dust particles in the Martian atmosphere away from a specific surface source, using a coupled system of a zonally symmetric primitive equation grid point model of the Martian atmosphere and an aerosol transport/microphysical model. Their findings include: (1) When the dust is distributed among a range of particle sizes from submicrons to tens of microns, there is a more extensive latitudinal transport away from a specified southern subtropical source than in the case when a single spherical particle size (2.5 μm) is used; (2) the input spherical particle size distribution inferred by Toon et al. (1977) from Mariner 9 IRIS spectra, is not maintained in suspension for an extended period of time at subsolar latitudes for radii between 1 and 10 μm; (3) when slower falling nonspherical (disk-shaped) particles are considered, an improved maintenance in suspension of the input particle size distribution is obtained, in better agreement with inferred values; and (4) the maximum calculate visible dust opacities at the latitudes of the Viking landers generally fall short of the values inferred during the 1977 global dust storms.

Planet-encircling dust storms do not occur during northern spring and summer seasons, even when there is an intense baroclinic zone adjacent to the north polar cap which produces local dust storms (Wolf et al., 1996). Figure 3 shows a local dust storm churning the edge of the Martian receding north polar cap. As pointed out by Zurek (1982), because of the ellipticity of the orbit of Mars and the present occurrence of aphelion in late northern spring, the insolation available at L_s near 20° is only 74% of that available at L_s near 200° during the present epoch. This reduces the intensity of the planetary-scale circulation and local convective activity.

9.2. MECHANISMS RELATED WITH EXPANSION OF VORTICAL MOTION

9.2.1. *Large Vortices*

Gierasch and Goody (1973) modified a terrestrial hurricane model, developed by Carrier (1971), to predict the evolution of a planet-encircling dust storm on Mars. They did so, considering that the planet-encircling storm of 1971 suggest a self-sustaining system converting solar to kinetic energy on a large organized scale. In the dust storm case the increase in enthalpy comes from absorption of solar radiation by the dust core, instead of by latent heat as in the case of terrestrial hurricanes. In this model, as adapted to Martian conditions, an axisymmetric swirling flow field is assumed to exist outside the central core and above the surface boundary layer (this might occur above an elevated plateau). The radial pressure gradient drives a flow radially inward toward the core where it rises. Then heating of the dusty core by absorption of solar radiation intensify the horizontal gradients of temperature at the core's periphery, accelerating the cyclonic swirling flow inward into the core. Above the core, there is a region where the flow is forced upward and outward from the core. Gierasch and Goody (1973) found that: (1) In the growth phase the area of the compact core of large dust particles grows by a factor of 10 in about 3 days, starting somewhere between 10^5 and 10^7 km^2. (2) In the mature phase the compact core exist for at least 10 more days, until day 13. At the same time a cloud of comparatively small dust particles spreads sideways covering the whole planet sometime after day 23. Particles 1 μm in diameter are convected up to 40 km. (3) In the decay phase gradual clearing takes place after days 13–23 with 1 μm particles finally clearing about day 140. They pointed out that these findings agree quite well with the observed behavior of the planet-encircling dust storm of 1971.

The local storms observed by Viking (e.g., Briggs et al., 1979) do not show vortical motions. The possible explanation is that the winds are relatively strong in the regions where the dust storms originate to allow the organization of the initial cyclonic swirling flow (Zurek, 1982).

9.2.2. *Dust Devils*

Dust devils have been proposed as a mechanism to rise dust into the Martian atmosphere (e.g., Ryan, 1964; Neubauer, 1966; Sagan and Pollack, 1969; Sagan et al., 1971). Ryan and Lucich (1983) made a study of local convective vortices (which includes dust devils) as observed by VL1 and VL2. By convective vortices the authors meant those that transport heat upward, being formed in the presence of superadiabatic temperature lapse rate and atmospheric vorticity. Ryan and Lucich found that: (1) convective vortices occurred more frequently during Martian spring and summer, (2) they occurred during the period from several hours after sunrise to few hours before sunset, (3) they were more common at the more southerly VL1 site where convection is expected to be more active, (4) in the majority of cases (about 70%) an increase in temperature was clearly associated with the vortex, (5) no preference in the formation of cyclone or anticyclone vortices was detected, and

(6) seven of the 118 vortices recorded had wind speeds that may have risen dust from the surface.

Dust devils have been detected from Viking Orbiter images by Thomas and Gierasch (1985). The overall shapes of the observed clouds (identified by those authors as dust devils) were columnar, cone, funnel, or irregular, and they were generally four to ten times as high as their were wide. The heights of most of the clouds (61 of 99 observations) were in the 1.0–2.5 km range; the maximum height was 6.8 km. The bases of the clouds were apparently narrow, and the widest areas near the tops of the clouds were about 1 km across. In addition, Thomas and Gierash have pointed out that all clouds identified as dust devils were imaged at 14 to 15 hours local time in local summer. Dust devils have also been detected analysing Pathfinder's meteorological data (Schofield et al., 1997).

The coexistence of a number of dust devils has been postulated as a mechanism which may produce local dust storms (Hess, 1973). Once a dust cloud at least 10 km thick and several tens of km in radius is formed by the dust devils, the absorption of solar radiation generate temperature gradients which, in turn, produce winds capable of rising more dust (Hess, 1973; Golitsyn, 1973).

10. Seasonal and Long-Term Aspects of the Dust Cycle

Although it is not the purpose of this article to discuss all the different aspects of the dust cycle on Mars, some seasonal and long-term aspects of the dust cycle should be briefly mentioned. A detailed discussion of this subject is given by Kahn et al. (1992).

Dust can be raised over large areas of Mars and redistributed over a large part of the planet during the occurrence of planet-encircling dust storms. In the years when planet-encircling dust storms are formed during southern hemisphere's summer, the dust raised in the southern hemisphere subtropics is transported to the northern hemisphere subtropics by large-scale cross-equatorial upper level winds associated with a Hadley type circulation (Kahn et al., 1992). Baroclinic waves in the northern hemisphere may transport dust toward the northern polar region (Tillman et al., 1979; Barnes et al., 1993). The incorporation of dust into the residual north polar cap was proposed by Pollack et al. (1979). This suggests that the northern polar region may act as a sink of dust in the present epoch. Other possible long-term sinks of dust during the current epoch, associated with the descending branch of the Hadley circulation, are the bright, low-thermal-inertia regions of Arabia, Tharsis, and Elysium in the northern hemisphere (Kahn et al., 1992). It is unlikely that the south polar cap may be a sink of dust in the present epoch, since in southern hemisphere's winter condensation is taking place at the south polar cap and transient baroclinic eddy activity is much weaker than in northern hemisphere's winter (Barnes et al., 1993). On the other hand, the more frequent formation of dust storms in some specific areas (southern hemisphere subtropics and near the retreating polar

cap-edges) indicate that these regions may be net sources of airborne dust (Kahn et al., 1992).

Transport of dust may also take place in periods when planet-encircling storms are not observed, as suggested by changes in surface albedo. The dust deposited in some regions may be transported by winds close to the surface to neighboring regions, which can explain changes in surface albedo. In general, changes in surface albedo can be explained by seasonal and interannual redistribution of very small amounts of dust (Kahn et al., 1992).

As pointed out by Kahn et al. (1992), if some regions are long-term sources or sinks, losing or gaining the equivalent of a few μm a year, meters of material can be removed or accumulated on time scales of 1 Myr. The observed polar- and low-latitude layered terrains indicate a net deposition of airborne dust. Since the obliquity cycle of Mars is about 51,000 years, the season of perihelion (when maximum insolation occurs) will reverse about every 25,000 years. This implies that in the next reverse of the obliquity cycle the present sink regions (at the northern low-latitudes and the northern polar region) will become source regions and the southern polar region will act as a sink for airborne dust. However, arguments given by Kahn et al. (1992) in relation to long-term dust deposition rates suggest that either the dust cycle has operated differently in the past or/and that the current understanding of the dust cycle is incomplete.

11. Concluding Remarks

The above description shows that important results have been obtained concerning the preponderant forcing mechanisms controlling the origen, maintainence, and decay of the dust storms. Nevertheless, further research is needed to provide additional information related to these systems. New missions to Mars would provide valuable observational data to evaluate the numerical model results.

Acknowledgments

The helpful suggestions and comments of an anonymous referee improved the manuscript and are greatly appreciated.

References

Antoniadi, E. M.: 1930, *La Planète Mars 1659–1929*, Hermann et Cie, Paris, pp. 39–47.

Bagnold, R. A.: 1941, *The Physics of Blown Sand and Desert Dunes*, Methuen, London, 265 pp.

Barnes, J. R., Pollack, J. B., Haberle, R. M., Leovy, C. B., Zurek, R. W., Lee, H., and Schaeffer, J.: 1993, 'Mars Atmospheric Dynamics as Simulated by the NASA Ames General Circulation Model, 2. Transient Baroclinic Eddies', *J. Geophys Res.* **98**, 3125–3148.

Blumsack, S. L. and Gierasch, P. J.: 1972, 'Mars: the Effects of Topography on Baroclinic Instability', *J. Atmos. Sci.* **29**, 1081–1089.

Blumsack, S. L., Gierasch, P. J., and Wessel, W. R.: 1973, 'An Analytical and Numerical Study of the Martian Planetary Boundary Layer Over Slopes', *J. Atmos. Sci.* **30**, 66–82.

Briggs, G. A., Baum, W. A., and Barnes, J.: 1979, 'Viking Orbiter Imaging Observations of Dust in the Martian Atmosphere', *J. Geophys. Res.* **84**, 2795–2820.

Burk, S. D.: 1976, 'Diurnal Winds Near the Martian Polar Caps', *J. Atmos. Sci.* **33**, 923–939.

Capen, C. F.: 1974, 'A Martian Yellow Cloud, July 1971', *Icarus* **22**, 345–362.

Carrier, G. F.: 1971, 'The Intensification of Hurricanes', *J. Fluid Mech.* **49**, 145–158.

Christensen, P. R.: 1986, 'Regional Dust Deposits on Mars: Physical Properties, Age, and History', *J. Geophys. Res.* **91**, 3533–3545.

Chylek, P. and Grams, G. W.: 1978, 'Scattering by Nonspherical Particles and Optical Properties of Martian Dust', *Icarus* **36**, 198–203.

Clancy, R. T. and Lee, S. W.: 1991, 'A New Look at Dust and Clouds in the Mars Atmosphere: Analysis of Emission-Phase-Function Sequences from Global Viking IRTM Observations', *Icarus* **93**, 135–158.

Clancy, R. T., Muhleman, D. O., and Berge, G. L.: 1990, 'Global Changes in the 0–70 km Thermal Structure of the Mars Atmosphere Derived from 1975–1989 Microwave CO spectra', *J. Geophys. Res.* **95**, 14543–14554.

Clancy, R. T., Lellouch, T. E., Billawala, Y. N., Sandor, B. J., and Rudy, D. J.: 1994, 'Microwave Observations of a 1994 Mars Global Dust Storm', *Bull. Am. Astron. Soc.* **26**, 1130.

Clancy, R. T., Lee, S. W., Gladstone, G. R., McMillan, W. W., and Rousch, T.: 1995, 'A New Model for Mars Atmospheric Dust Based Upon Analysis of Ultraviolet Through Infrared Observations from Mariner 9, Viking, and Phobos', *J. Geophys. Res*. **100**, 5251–5263.

Clancy, R. T., Grossman, A. W., Wolf, M. J., James, P. B., Rudy, D. J., Billawala, Y. N., Sandor, B. J., Lee, S. W., and Muhleman, D. O.: 1996, 'Water Vapor Saturation at Low Altitudes Around Mars Aphelion: A Key to Mars Climate?', *Icarus* **122**, 36–62.

Conrath, B. J.: 1975, 'Thermal Structure of the Martian Atmosphere During the Dissipation of the Dust Storm of 1971', *Icarus* **24**, 36–46.

Conrath, B., Curran, R., Hanel, R., Kunde, V., Maguire, W., Pearl, J., Pirraglia, J., Welker, J., and Burke, T.: 1973, "Atmospheric and Surface Properties of Mars Obtained by Infrared Spectroscopy on Mariner 9", *J. Geophys. Res.* **78**, 4267–4278.

Csanady, G. T.: 1967, 'On the "Resistance Law" of a Turbulent Ekman Layer', *J. Atmos. Sci.* **24**, 467–471.

Dollfus, A., Bowell, E., and Ebisawa, S.: 1984a, 'Polarimetric Analysis of the Martian Dust Storms and Clouds in 1971', *Astron. Astrophys.* **131**, 123–136.

Dollfus, A., Bowell, E., and Ebisawa, S.: 1984b, 'The Martian Dust Storms of 1973: A Polarimetric Analysis', *Astron. Astrophys.* **134**, 343–353.

Drossart, P., Rosenqvist, J., Erard, S., Langevin, Y., Bibring, J.-P., and Combes, M.: 1991, 'Martian Aerosol Properties from the Phobos ISM Experiment', *Ann. Geophys.* **9**, 754–760.

Ebisawa, S. and Dollfus, A.: 1986, 'Martian Dust Storms at the Early Stage of Their Evolution', *Icarus* **66**, 75–82.

Edgett, K. S. and Christensen, P. R.: 1991, 'The Particle Size of Martian Aeolian Dunes', *J. Geophys. Res.* **96**, 22,765–22,776.

Fernández, W.: 1995a, 'Description of the Martian Polar Cap Breeze', *Earth, Moon, and Planets* **70**, 183–191.

Fernández, W.: 1995b, 'A Numerical Simulation of the Martian Polar Cap Breeze', *Earth, Moon, and Planets* **70**, 193–205.

French, R. G. and Gierasch, P. J.: 1979, The Martian Polar Vortex: Theory of Seasonal Variation and Observations of Eolian Features', *J. Geophys. Res.* **84**, 4634–4642.

Gierasch, P. J.: 1974, 'Martian Dust Storms', *Rev. Geophys. Space Phys.* **12**, 730–734.

Gierasch, P. J. and Goody, R. M.: 1972, 'The Effect of Dust on the Temperature of the Martian Atmosphere', *J. Atmos. Sci.* **29**, 400–402.

Gierasch, P. J. and Goody, R. M.: 1973, 'A Model of a Martian Great Dust Storm', *J. Atmos. Sci.* **30**, 169–179.

Gifford, F. A.: 1964, 'A Study of Martian Yellow Clouds that Display Movement', *Mon. Wea. Rev.* **92**, 435–439.

Golytsyn, G. S.: 1973, 'On the Martian Dust Storms', *Icarus* **18**, 113–119.

Greeley, R., Leach, R., White, B. R., Iversen, J. D., and Pollack, J. B.: 1980, 'Threshold Wind Speeds for Sand on Mars: Wind Tunnel Simulations', *Geophys. Res. Lett.* **7**, 121–124.

Greeley, R., Lancaster, N., Lee, S., and Thomas, P.: 1992, 'Martian Aeolian Processes, Sediments and Features', in H. H. Kieffer, B. M. Jakosky, C. W. Snyder, and M. S. Matthews (eds.), *Mars*, University of Arizona Press, Tucson, Arizona, pp. 730–766.

Haberle, R. M.: 1979, 'The Influence of the Martian Polar Caps on the Diurnal Tide', *Icarus* **39**, 184–191.

Haberle, R. M. and Jakosky, B. M.: 1991, 'Atmospheric Effects on the Remote Determination of Thermal Inertia on Mars', *Icarus* **90**, 187–204.

Harberle, R. M., Leovy, C. B. and Pollack, J. B.: 1979, 'A Numerical Model of the Martian Polar Cap Winds', *Icarus* **39**, 151–183.

Haberle, R. M., Leovy, C. B., and Pollack, J. B.: 1982, 'Some Effects of Global Dust Storms on the Atmospheric Circulation on Mars', *Icarus* **50**, 322–367.

Haberle, R. M., Pollack, J. B., Barnes, J. R., Zurek, R. W., Leovy, C. B., Murphy, J. R., Lee, H., and Schaeffer, J.: 1993, 'Mars Atmospheric Dynamics as Simulated by the NASA Ames General Circulation Model, 1. The Zonal Mean Circulation', *J. Geophys. Res.* **98**, 3093–3123.

Hanel, R. A., Conrath, B. J., Hovis, W. A., Kunde, V. G., Lowman, P. D., Pearl, J. C., Prabhakara, C., and Schlachman, B.: 1972, 'Infrared Spectroscopy Experiment on the Mariner 9 Mission: Preliminary Results', *Science* **175**, 305–308.

Hartmann, W. K. and Price, M. J.: 1974, 'Mars: Clearing of the 1971 Dust Storm', *Icarus* **21**, 28–34.

Hess, S. L.: 1973, "Martian Winds and Dust Clouds", *Planetary Space Sci.* **21**, 1549–1557.

Hunt, G. E., Mitchell, E. A., and Peterfreund, A. R.: 1980, 'The Opacity of Some Local Martian Dust Storms Observed by the Viking IRTM', *Icarus* **41**, 389–399.

Ingersoll, A. P. and Lyons, J. R.: 1993, 'Mars Dust Storms: Interannual Variability and Chaos', *J. Geophys. Res.* **98**, 10,951–10,961.

Iversen, J. D., Pollack, J. B., Greeley, R., and White, B. R.: 1976a, "Saltation Threshold on Mars: The Effect of Interparticle Force, Surface Roughness, and Low Atmospheric Density', *Icarus* **29**, 381–393.

Iversen, J. D., Greeley, R., and Pollack, J. B.: 1976b, 'Windblown Dust on Earth, Mars, and Venus', *J. Atmos. Sci.* **33**, 2425–2429.

James, P. B.: 1985, 'Martian Local Dust Storms', in G. Hunt (ed.), *Recent Advances in Planetary Meteorology*, Cambridge University Press, New York, pp. 85–100.

James, P. B. and Evans, N.: 1981, 'A Local Dust Storm in the Chryse Region of Mars: Viking Orbiter Observations', *Geophys. Res. Lett.* **8**, 903–906.

Jaquin, F., Gierasch, P., and Kahn, R.: 1986, 'The Vertical Structure of Limb Hazes in the Martian Atmosphere', *Icarus* **68**, 442–461.

Kahn, R. A., Martin, T. Z., Zurek, R. W., and Lee, S. W.: 1992, 'The Martian Dust Cycle', in H. H. Kieffer, B. M. Jakosky, C. W. Snyder and M. S. Matthews (eds.), *Mars*, University of Arizona Press, Tucson, Arizona, pp. 1017–1053.

Kieffer, H. H., Chase Jr., S. C., Miner, E., Münch, G., and Neugebauer, G.: 1973, 'Preliminary Report on Infrared Radiometric Measurements from the Mariner 9 Spacecraft', *J. Geophys. Res*. **78**, 4291–4312.

Leovy, C. and Mintz, Y.: 1969, 'Numerical Simulation of the Atmospheric Circulation and Climate of Mars', *J. Atmos. Sci.* **26**, 1167–1190.

Leovy, C. B. and Zurek, R. W.: 1979, 'Thermal Tides and Martian Dust Storms: Direct Evidence for Coupling', *J. Geophys. Res.* **84**, 2956–2968.

Leovy, C. B., Briggs, G., Young, A., Smith, B., Pollack, J., Shipley, E., and Wildey, R.: 1972, 'The Martian Atmosphere: Mariner 9 Television Experiment Progress Report', *Icarus* **17**, 373–393.

Leovy, C. B., Zurek, R. W., and Pollack, J. B.: 1973, 'Mechanisms for Mars Dust Storms', *J. Atmos. Sci.* **30**, 749–762.

Magalhaes, J. and Gierasch, P.: 1982, 'A Model of Martian Slope Winds: Implications for Eolian Transport', *J. Geophys. Res.* **87**, 9975–9984.

Martin, L. J.: 1974a, 'The Major Martian Yellow Storm of 1971', *Icarus* **22**, 175–188.

Martin, L. J.: 1974b, 'The Major Martian Dust Storms of 1971 and 1973', *Icarus* **23**, 108–115.

Martin, L. J.: 1976, '1973 Dust Storm on Mars: Maps from Hourly Photographs', *Icarus* **29**, 363–380.

Martin, L. J.: 1984, 'Clearing the Martian Air: The Troubled History of Dust Storms', *Icarus* **57**, 317–321.

Martin, L. J. and Zurek, R. W.: 1993, 'An Analysis of the History of Dust Activity on Mars', *J. Geophys. Res.* **98**, 3221–3246.

Martin, L. J., Beish, J. D., and Parker, D. C.: 1991a, 'Martian Dust Storms in 1990', *Bull. Am. Astron. Soc.* **23**, 1217.

Martin, L. J., James, P. B., and Zurek, R. W.: 1991b, 'Observed Changes in Limb Clouds Immediately Prior to the Onset of Planet-Encircling Dust Storms', in *MSATT Workshop on the Martian Surface and Atmosphere through Time*, Lunar and Planetary Institute, Houston, Texas, p. 86.

Martin, T. Z.: 1986, 'Thermal Infrared Opacity of the Mars Atmosphere', *Icarus* **66**, 2–21.

Martin, T. Z.: 1995, 'Mass of Dust in the Martian Atmosphere', *J. Geophys. Res.* **100**, 7509–7512.

Martin, T. Z. and Richardson, M. I.: 1993, 'New Dust Opacity Mapping from Viking Infrared Thermal Mapper Data', *J. Geophys. Res.* **98**, 10941–10949.

Martin, T., Peterfreund, A., Miner, E., Kieffer, H., and Hunt, G.: 1979, 'Thermal Infrared Properties of the Martian Atmosphere. 1. Global Behavior at 7, 9, 11, and 20 μm', *J. Geophys. Res.* **84**, 2830–2842.

Moore, H. J.: 1985, 'The Martian Dust Storm of Sol 1742', *J. Geophys Res.* **90**, Supplement, D163–D174.

Moroz, V. I. and Ksanfomaliti, L. V.: 1972, "Preliminary Results of Astrophysical Observations of Mars from Mars 3', *Icarus* **17**, 408–422.

Murphy, J. R., Toon, O. B., Haberle, R. M., and Pollack, J. B.: 1990, 'Numerical Simulations of the Decay of Martian Global Dust Storms', *J. Geophys. Res.* **95**, 14,629–14,648.

Murphy, J. R., Haberle, R. M., Toon, O. B., and Pollack, J. B.: 1993, 'Martian Global Dust Storms: Zonally Symmetric Numerical Simulations Including Size-Dependent Particle Transport', *J. Geophys. Res.* **98**, 3197–3220.

Neubauer, F. M.: 1966, 'Thermal Convection in the Martian Atmosphere', *J. Geophys. Res.* **71**, 2419–2426.

Ockert-Bell, M. E., Bell III, J. F., Pollack, J. B., McKay, C. P., and Forget, F.: 1997, 'Absorption and Scattering Properties of the Martian Dust in the Solar Wavelengths', *J. Geophys. Res.* **102**, 9039–9050.

Paige, D. A., Herkenhoff, H. E., and Murray, C. B.: 1987, 'Martian Dust Properties from Mariner 9 IRIS Observations of the South Polar Cap', *Bull. Am. Astron. Soc.* **19**, 815.

Pallmann, A. J. and Frisella, S. P.: 1972, 'Numerical Simulation of Radiative-Conductive Heat Transfer in the Martian Atmosphere-Polar Cap Utilizing Mariner 9 IRIS Data', *Conference on Atmospheric Radiation*, August 7–9, Fort Collins, Colorado; published by AMS, Boston, Mass.

Pallmann, A. J., Dannevik, W. P., and Frisella, S. P.: 1973, 'Martian Thermal Boundary Layers: Subhourly Variations Induced by Radiative-Conductive Heat Transfer within the Dust-Laden Atmosphere-Ground System', NASA Contractor Report, Washington, D.C.

Pang, K. and Hord, C. W.: 1973, 'Mariner 9 Ultraviolet Spectrometer Experiment: 1971 Dust Storm', *Icarus* **18**, 481–488.

Pank, K., Ajello, J. M., Hord, C. W., and Egan, W. G.: 1976, 'Complex Refractive Index of Martian Dust: Mariner 9 Ultraviolet Observations', *Icarus* **27**, 55–67.

Peterfreund, A. R.: 1981, 'Visual and Infrared Observations of Wind Streaks on Mars', *Icarus* **45**, 447–467.

Pollack, J., Colburn, D., Kahn, R., Hunter, J., Van Camp, W., Carlston, C., and Wolfe, M.: 1977, 'Properties of Aerosols in the Martian Atmosphere as Inferred from Viking Lander Imaging Data', *J. Geophys. Res.* **82**, 4479–4496.

Pollack, J., Colburn, D., Flasar, F. M., Kahn, R., Carlston, C., and Pidek, D.: 1979, 'Properties and Effects of Dust Particles Suspended in the Martian Atmosphere', *J. Geophys. Res.* **84**, 2929–2945.

Pollack, J. B., Haberle, R. M., Schaeffer, J., and Lee, H.: 1990, 'Simulations of the General Circulation of the Martian Atmosphere 1. Polar Processes', *J. Geophys. Res.* **95**, 1447–1474.

Pollack, J. B., Haberle, R. M., Murphy, J. R., Schaeffer, J., and Lee, H.: 1990, 'Simulations of the General Circulation of the Martian Atmosphere 2. Seasonal Pressure Variations', *J. Geophys. Res.* **95**, 3149–3181.

Pollack, J. B., Ockert-Bell, M. E., and Shepard, M. K.: 1995, 'Viking Lander Image Analysis of Martian Atmospheric Dust', *J. Geophys. Res.* **100**, 5235–5250.

Presley, M. A. and Christensen, P. R.: 1997a, 'Thermal Conductivity Measurements of Particulate Materials, 1, A Review', *J. Geophys. Res.* **102**, 6535–6549.

Presley, M. A. and Christensen, P. R.: 1997b, 'Thermal Conductivity Measurements of Particulate Materials, 2, Results', *J. Geophys. Res.* **102**, 6551–6566.

Presley, M. A. and Christensen, P. R.: 1997c, 'The Effect of Bulk Density and Particulate Size Sorting on the Thermal Conductivity of Particulate Materials Under Martian Atmospheric Pressures', *J. Geophys. Res.* **102**, 9221–9229.

Ryan, J. A.: 1964, 'Notes on the Martian Yellow Clouds', *J. Geophys. Res.* **69**, 3759–3770.

Ryan, J. A. and Henry, R. M.: 1979, 'Mars Atmospheric Phenomena During Major Dust Storms, as Measured at Surface', *J. Geophys. Res.* **84**, 2821–2829.

Ryan, J. A. and Lucich, R. D.: 1983, 'Possible Dust Devils, Vortices on Mars', *J. Geophys. Res.* **88**, 11,005–11,011.

Ryan, J. A. and Sharman, R. D.: 1981, 'Two Major Dust Storms, One Mars Year Apart: Comparison from Viking Data', *J. Geophys. Res.* **86**, 3247–3254.

Ryan, J. A., Henry, R. M., Hess, S. L., Leovy, C. B., Tilllman, J. E., and Walcek, C.: 1978, 'Mars Meteorology: Three Seasons at the Surface', *Geophys. Res. Lett.* **5**, 715–718.

Ryan, J. A., Sharman, R. D., and Lucich, R. D.: 1981, 'Local Mars Dust Storm Generation Mechanism', *Geophys. Res. Lett.* **8**, 899–901.

Sagan, C. and Pollack, J. B.: 1967, 'A Winblown Dust Model of Martian Surface Features and Seasonal Changes', Smithsonian Astrophysical Observatory, Special Report 255, Cambridge, Mass.

Sagan, C. and Pollack, J. B.: 1969, 'Windblown Dust on Mars', *Nature* **223**, 791–794.

Sagan, C., Veverka, J., and Gierasch, P.: 1971, 'Observational Consequences of Martian Wind Regimes', *Icarus* **15**, 253–278.

Sagan, C., Veverka, J., Fox, P., Dubisch, R., French, R., Gierasch, P., Quam, L., Lederberg, J., Levinthal, E., Tucker, R., Eross, B., and Pollak, J.: 1973, 'Variable Features on Mars. 2. Mariner 9 Global Results', *J. Geophys. Res.* **78**, 4163–4196.

Santee, M. and Crisp, D.: 1992, 'Atmospheric and Surface Temperatures and Airborne Dust from Mariner 9 IRIS Data', in R. M. Haberle et al. (eds.), *Workshop on the Martian Surface and Atmosphere Through Time (MSATT)*, LPI Tech. Rep. 92-02, Lunar and Planetary Institute, Houston, pp. 128–130.

Santee, M. and Crisp, D.: 1993, 'Thermal Structure of Dust Loading of the Martian Atmosphere During Late Southern Summer: Mariner 9 Revisited', *J. Geophys. Res.* **98**, 3261–3279.

Schneider, E. K.: 1983, 'Martian Great Dust Storms: Interpretive Axially Symmetric Models', *Icarus* **55**, 302–331.

Schofield, J. T., Barnes, J. R., Crisp, D., Haberle, R. M., Larsen, S., Magalhaes, J. A., Murphy, J. R., Seiff, A., and Wilson, G.: 1997, 'The Mars Pathfinder Atmospheric Structure Investigation/Meteorology (ASI/MET) Experiment', *Science* **278**, 1752–1758.

Smith, P. H., Bell III, J. F., Bridges, N. T., Britt, D. T., Gaddis, L., Greeley, R., Keller, H. U., Herkenhoff, K. E., Jaumann, R., Johnson, J. R., Kirk, R. L., Lemmon, M., Maki, J. N., Malin, M. C., Murchie, S. L., Oberst, J., Parker, T. J., Reid, R. J., Sablotny, R., Soderblom, L. A., Stoker, C., Sullivan, R., Thomas, N., Tomasko, M. G., Ward, W., and Wegryn, E.: 1997, 'Results from the Mars Pathfinder Camera', *Science* **278**, 1758–1765.

Thomas, P. and Gierasch, P. J.: 1985, 'Dust Devils on Mars', *Science* **230**, 175–177.

Thorpe, T. E.: 1978, 'Viking Orbiter Observations of the Mars Opposition Effect', *Icarus* **36**, 204–215.

Thorpe, T. E.: 1981, 'Mars Atmospheric Opacity Effects Observed in the Northern Hemisphere by Viking Orbiter Imaging', *J. Geophys. Res.* **86**, 11,419–11,429.

Tillman, J. E., Henry, R. M., and Hess, S. L.: 1979, 'Frontal Systems During Passage of the Martian North Polar Hood over the Viking Lander 2 Site Prior to the First 1977 Dust Storm', *J. Geophys. Res.* **84**, 2947–2955.

Toon, O. B., Pollack, J. B., and Sagan, C.: 1977, 'Physical Properties of the Particles Composing the Martian Dust Storm of 1971–72', *Icarus* **30**, 663–696.

Wolf, M. J., Lee, S. W., Clancy, R. T., Martin, L. J., Bell III, J. F., and James, P. B.: 1997, '1995 Observations of Martian Dust Storms Using Hubble Space Telescope', *J. Geophys. Res.* **102**, 1679–1692.

Zurek, R. W.: 1981, 'Inference of Dust Opacities for the 1977 Martian Great Dust Storms from Viking Lander 1 Pressure Data', *Icarus* **45**, 202–215.

Zurek, R. W.: 1982, 'Martian Great Dust Storms: An Update', *Icarus* **50**, 288–310.

Zurek, R. W., and Martin, L. J.: 1993, 'Interannual Variability of Planet-Encircling Dust Storms on Mars', *J. Geophys. Res.* **98**, 3247–3259.

Zurek, R. W., Barnes, J. R., Haberle, R. M., Pollack, J. B., Tillman, J. E., and Leovy, C. B.: 1992, 'Dynamics of the Atmosphere of Mars', in H. H. Kieffer, B. M. Jakosky, C. W. Snyder and M. S. Matthews (eds.), *Mars*, University of Arizona Press, Tucson, Arizona, pp. 835–933.